

UV-vis electron absorption spectral modeling

The spectral modeling was developed on the basis of the coordination chemical principles of weak field Fe-S cluster chemistry. A good review of weak-field Fe-S complexes can be found by [Holm et al. DOI: 0.1021/cr020615+](#).

1. Mononuclear, rubredoxin-like Fe thiolate complexes

In our reconstitution experiments, the $[\text{Fe}(\text{SR})_4]^{2-}$, rubredoxin like complexes are considered as unwanted, byproducts given that we are exclusively focused on $[\text{4Fe-4S}]$ -maquettes. However, these complexes provide a simple and clear first step for the development of the spectral model. UV-vis or electronic absorption spectroscopy is a valence excited state technique, which utilizes the 200 – 800 nm ($12,500 - 50,000 \text{ cm}^{-1}$) region of electromagnetic radiation. This energy range allows for the excitation of electrons from the occupied to the unoccupied frontier orbitals in the $\sim 1.5 - 6.2 \text{ eV}$ energy window. For transition metal complexes, assuming innocent coordination environment and normal M-L chemical bonding, the frontier orbitals are dominantly metal d-orbital based. A simple bonding model that is already insightful is ligand field theory which considers explicitly the metal d-orbitals and implicitly the ligand environment through the Racah parameters.

The ligand field splitting for a weak field coordination environment of a transition metal ion is small due to the σ - and π -donation of the ligand (thiolates). The ideal tetrahedral splitting is shown in Figure 1 with the symmetry labels of the orbitals. The small ligand field splitting (Δ) practically renders the d-orbitals behave as atomic orbitals at the weak field limit and thus Hund's rule apply, i.e. 1) max m_s and 2) max m_l quantum numbers. This renders the complexes high spin (Figure 2).

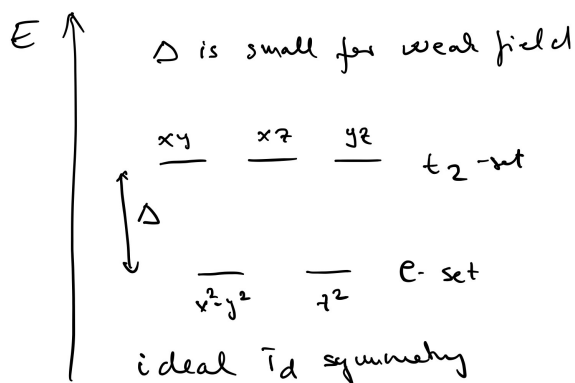


Figure 1. T_d ligand field splitting

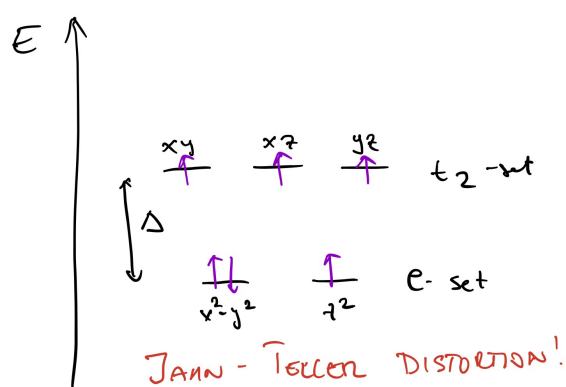


Figure 2. High spin d^6 configuration

Considering the occupation of the d-orbital of the central ion, even in the case of homoleptic complex such as the rubredoxin-like tetrathiolate complex, the symmetrical orbital splitting may be distorted for non-degenerate occupation of energetically degenerate orbitals (Jahn-Teller distortion force lowering the electronic energy). However, since both distortions shown in Figure 3 are equally possible, the

molecular structure and even the room temperature spectra will actually not display the results of the distortion (dynamic Jahn-Teller effect) other than broadening of the spectral features.

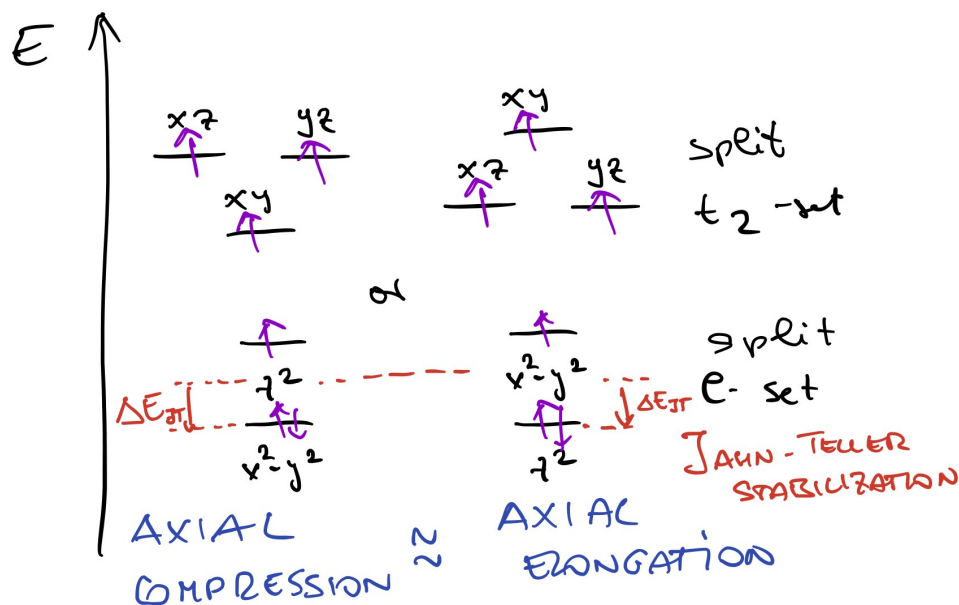


Figure 3. Equivalent electronic distortions (dynamic JT) of the ligand-field for d^6 tetrahedral complexes.

In the ligand-field set, the only allowed excitation involves the spin-down (β) electron in the lowest lying d-orbital into any of the higher lying vacant β -electron holes. Notably, the excitation energy within the e-set will be independent from the ligand field strength, while it can be a measure of the Jahn-Teller distortion force, if resolved. The $e \rightarrow t_2$ excitation is the so-called $d \rightarrow d$ or ligand-field transitions (LFT), which commonly occur at longer wave length region of the UV-vis, often in the near-IR region.

Now considering non-metal based orbitals below and above the ligand field set (Figure 4) we can define all possible excitations that we will model by fitting the UV-vis spectra. For the sake of generality, the degeneracy of d-orbitals are lifted as expected for the rubredoxin-like Fe-thiolate complex, given that the Fe-S(thiolate) bond rotation will eliminate the symmetry of the coordination environment.

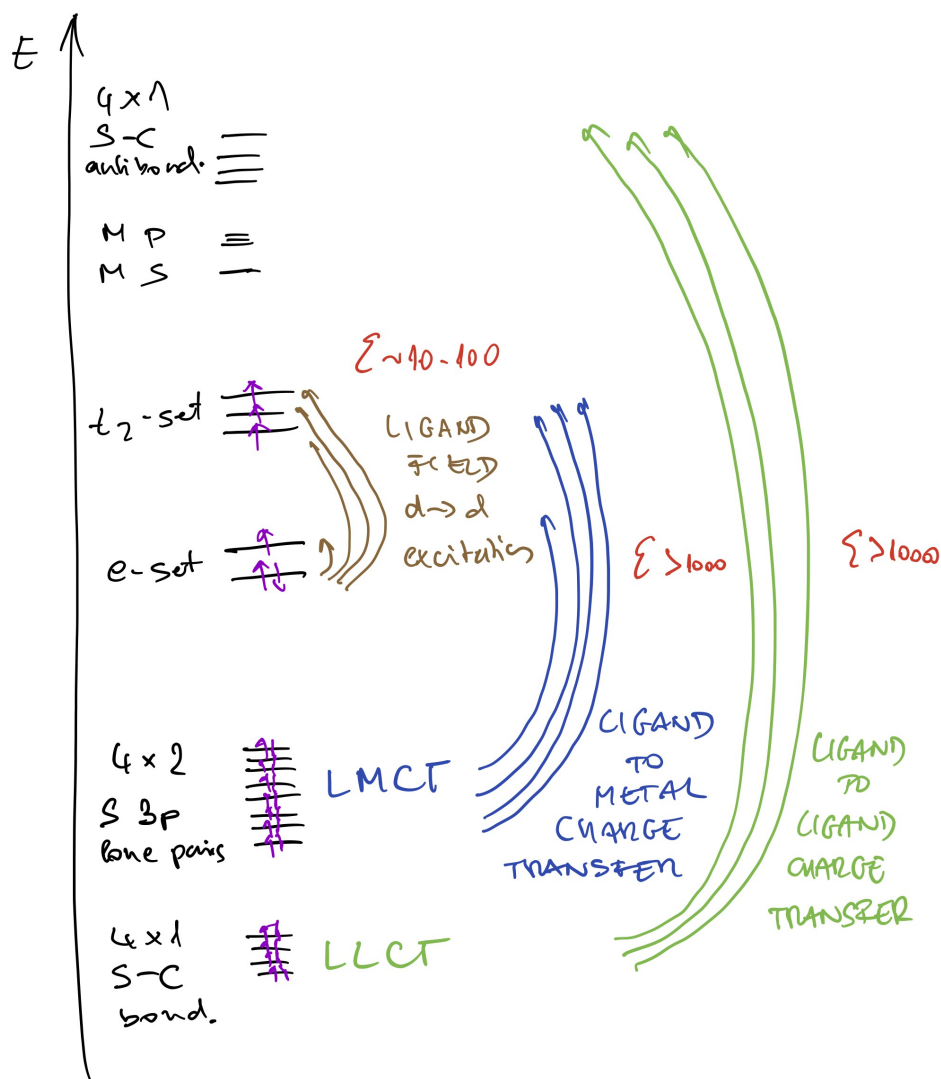


Figure 4. Complete molecular orbital energy diagram of the [Fe(SR)₄] complex

The molar extinction coefficients (oscillator strength) and the excitation energies clearly classify the various adsorption bands that can be used (as envelop of numerous excitations) to fit and model the spectral features of rubredoxin-like, mononuclear Fe-thiolate complexes.

2. Multinuclear, Fe-S clusters with thiolate ligands (ferredoxins)

Building on the above electronic structure model we can extend the molecular orbital diagram of the mononuclear Fe-thiolate complex by considering a new ligand environment as created by the sulfide ions. Sulfides are even more weak field ligands than the S(thiolate) due to the availability of three S 3p² lone pairs for σ - and π -donation to both Fe centers they are connected to (Figure 5).

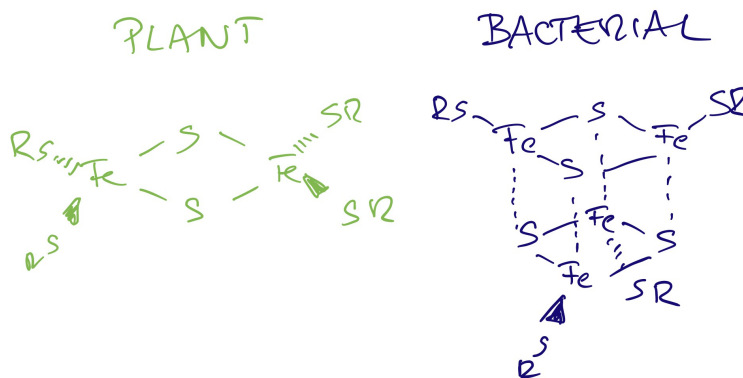


Figure 5: Fe-S clusters of plant and bacterial ferredoxins

For the construction of the molecular orbital diagram, it is important to consider the effective nuclear charge of the S atoms seen by the S 3p orbitals in the sulfide and in the thiolate. Due to the more negative charge of the sulfides, its 3p-based lone pairs are located at higher energy than the lone pairs of the S(thiolate). Thus, the LMCT bands in of Figure 4 will split into two groups; the lower energy will correspond to the sulfide \rightarrow Fe while the higher energy will be due to thiolate $S \rightarrow$ Fe charge transfers. Figure 6 shows the basis of the spectral modeling that we will use for quantitation of the [4Fe-4S]-maquette reconstitution yields.

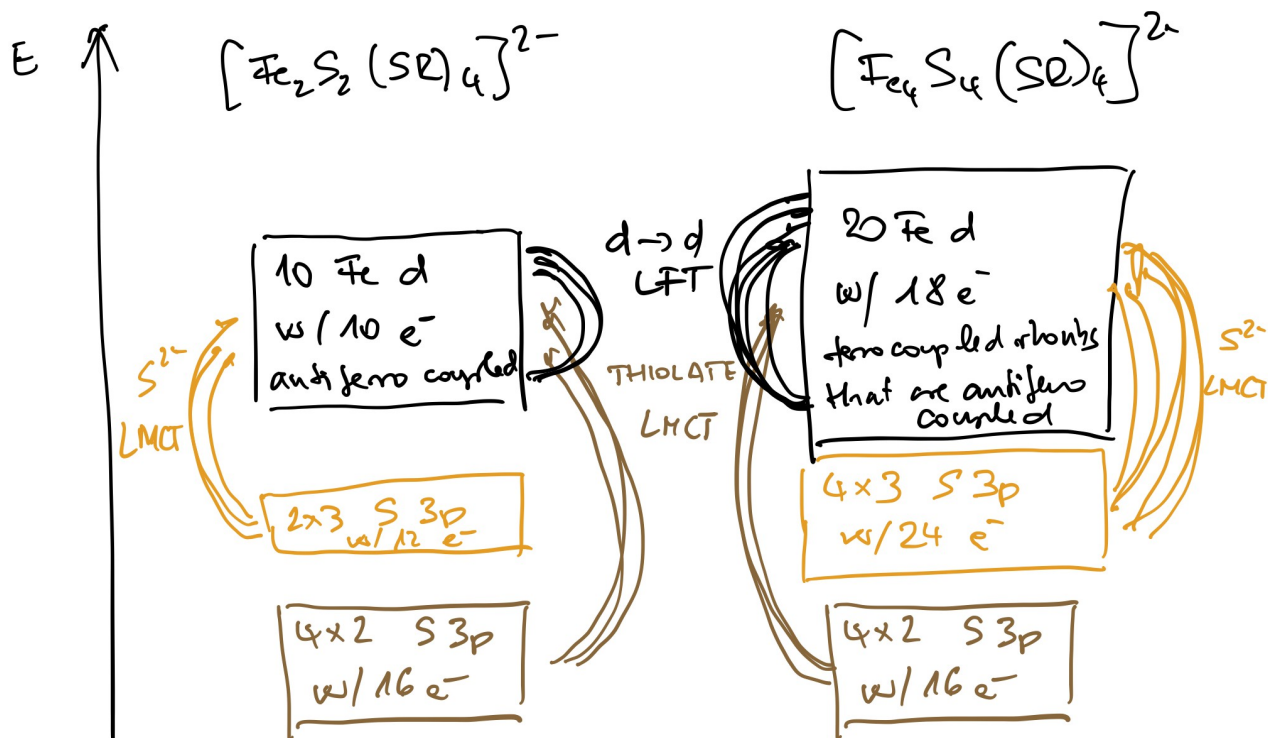


Figure 6. Schematic blocks of sulfide and thiolate donor and Fe-based acceptor orbitals

Thus, the UV-vis modeling will be accomplished by representative fits to the following features

- 1) low energy, weak ($\epsilon \approx 10$) $d \rightarrow d$ LFT with one broad envelop

- 2) intermediate energy, strong ($\epsilon \approx 10^3$) LMCT associated with sulfides \rightarrow Fe
- 3) high energy, strong ($\epsilon \approx 10^3$) LMCT associated with thiolate S \rightarrow Fe
- 4) at the low λ limit of the UV-vis range strong ($\epsilon \approx 10^5$) LLCT or LL'CT associated with sulfide/thiolates

Caveats:

- 1) due to the presence of $\text{FeS}_{(\text{aq})}$ nanoparticles ($\text{FeS}_{n < 150}$) which appears as turbidity at the high λ limit of the spectrum, the LFT feature cannot be used for analytical quantitation because this may significantly vary from sample to sample depending on the success of reconstitution experiment.
- 2) similarly at the high energy end, the LLCT or LL'CT excitations are ill-defined and these may “steal” intensity away from the thiolate LMCT band.
- 3) more caveats will be listed here as they are identified.

3. Fitting procedures

We have considered numerous fitting strategies to find an optimum number of peaks to describe the smooth, undulating features of the UV-vis spectra of [4Fe-4S]-maquettes. When the non-linear wave length scale is converted to the linear wave number scale, the features become broader and the fitting is even more challenging. Only 4 peaks as single features for $d \rightarrow d$ LFT, $S^{2-} \rightarrow$ Fe LMCT, $RS^- \rightarrow$ Fe LMCT, and LLCT does not give satisfactory fits due to the broad, envelop like features that cannot be described with a single Voigt line-shape. Any fits with less than 6 peaks (double for the LMCT features) did always result in high residuals or fits that were visibly not acceptable. Fits composed of more than 6 peaks cannot be justified due to the peak and shoulder resolution, since iterative peak fitting routinely collapsed into 6 peaks. The extra peaks formed small peaks under dominant ones. In the case of chemical speciation (presence of the rubredoxin-like feature) or high turbidity, additional peaks have to be introduced in order to maintain the validity of the 6-peak model.

The steps of our standard operating procedures for the UV-vis modeling are as follows:

1. obtain the CSV/DAT file from the spectrometer
2. since wavelength is NOT a linear scale, fitting needs be done in wavenumber scale; thus convert wavelength to wavenumber scale ($\tilde{\nu} = 1E7/\lambda(\text{in nm})$ gives $1/\text{cm}$ wavenumber)
3. for [PeakFit](#), which can only handle the old 2004-2007 Excel, save the spectrum to XLS format
4. open up the XLS file in [PeakFit](#) and prepare the data by cutting the spectrum down (apply to new) to 12,500 – 37,500 cm^{-1} range, which is was selected by considering the spectra of all [4Fe-4S]-maquettes in our sample library
5. select Fitting Method (I) that focuses on minimizing residuals
6. open up the 6-peaks_abs .scn template. The fit should already be fairly close, but the intensity likely be off depending on the success of the reconstitution process
7. although it is not absolutely needed, but iterative curve fitting procedure can be enhanced by

manually adjusting intensity of peaks or even gently the peak positions to achieve a better initial values for fitting; this also avoids shifting the peaks that may redistribute the peak intensities (adjacent peaks steal intensity from each other)

8. start fit once and use graphical update to see what is happening; generally the fitting finishes quick - save the fit to SCN file.
9. Start the fit again by requesting additional adjustment in order to evaluate how robust is the fit, whether there are peaks that collapse or whether more peaks needed due to speciation. If there are large scale changes, visually detectable intensity redistributions, the model needs to be rejected and the fit obtained in Step 8 needs to be used
10. review fit:
 - a) print fit as a postscript PS file that can be readily converted to PDF, use white background w/colored traces of components
 - b) export fit results to XLS for the extended range 11,000 – 40,000 using 5 cm⁻¹ fine steps
 - c) numerical results in TXT of the detailed summary of fitting
 - d) tabulate data in TAB: results of fit for every data point
 - e) print residuals as a postscript PS file, use white background w/colored traces of components
 - f) exit from review
11. save the fit to SCN file
12. save the truncated spectrum as .DAT file
13. open up the master spreadsheet `UV-vis.xlsx` and calculate the chromophore, [4Fe-4S]-maquette concentration relative to three standards from literature. Use the Integrated Area values instead of the Analytical Area, since the latter may reach outside of the 12,500 – 37,500 cm⁻¹ wave number range used for fitting. As shown on the top of the `UV-vis.xlsx` sheet, the numerical integrated area were used to convert the intensity values to concentration for the literature-based, reference compounds [Fe₄S₄(SEt)₄]²⁻ in acetonitrile [[DOI: 10.1021/ja00350a028](https://doi.org/10.1021/ja00350a028)], [Fe₄S₄(BME)₄]²⁻ in 2-(cyclohexylamino)ethanesulfonic acid buffered aqueous solution [[DOI: /10.1073/pnas.94.13.6635](https://doi.org/10.1073/pnas.94.13.6635)], and buffered aqueous solution of the as prepared, oxidized PFL-AE radical SAM metalloenzyme from the Broderick laboratory at MSU [[DOI: 10.1021/ja9711425](https://doi.org/10.1021/ja9711425)].

4. Demonstrative worked out example for the peptide-free reconstitution sample

Step 1

```

AKG_2_80_exp.csv
Baseline 100%T,,blank,,AKG_2_80_NoPep,
Wavelength (nm),Abs,Wavelength (nm),Abs,Wavelength (nm),Abs
800,0.106910378,800,-4.79E-05,800,0.092211105
799,0.106838428,799,-0.000153528,799,0.092428498
798,0.106648743,798,0.000347321,798,0.092960157
797,0.107060693,797,-3.63E-05,797,0.092660941
796,0.106768355,796,-2.54E-06,796,0.093095072
795,0.106247865,795,4.05E-05,795,0.093731321
794,0.105830342,794,-0.000122993,794,0.094315872
793,0.106235631,793,-0.000117144,793,0.094133824
792,0.105950818,792,-3.11E-05,792,0.094686538
791,0.105765745,791,-7.25E-05,791,0.095017985
790,0.105225608,790,-0.000152338,790,0.095648348
789,0.1049105,789,0.000281964,789,0.096166328
788,0.104982488,788,-0.000126719,788,0.096401222
787,0.104811639,787,4.68E-05,787,0.096597061
786,0.104180083,786,7.91E-05,786,0.097608618
785,0.103912301,785,0.000243888,785,0.097806066
784,0.104177386,784,-0.000105498,784,0.09774933
783,0.103992835,783,-0.000159635,783,0.098052107
782,0.103279099,782,-5.09E-05,782,0.099052362
781,0.102827251,781,0.000382141,781,0.099704012
780,0.103229024,780,-0.000131429,780,0.09947224
779,0.102866292,779,1.80E-05,779,0.099986911
778,0.102258131,778,-7.28E-05,778,0.100725874
777,0.10177011,777,-0.000133448,777,0.101264395
776,0.102120139,776,-7.87E-05,776,0.101201713
775,0.102074854,775,-0.00024414,775,0.101362914
774,0.101749949,774,-0.000230997,774,0.101820923
773,0.101064317,773,-9.07E-05,773,0.102763981
772,0.10119044,772,-0.000115436,772,0.102839291
771,0.100875147,771,-5.25E-05,771,0.103456311
770,0.100586906,770,-6.11E-05,770,0.103771709
769,0.099943705,769,-4.02E-05,769,0.104630373
768,0.100174725,768,-0.000162533,768,0.104671419
767,0.099929564,767,-0.000138571,767,0.105079651
766,0.099638753,766,-1.28E-05,766,0.105538994
-----

```

Step 2

	A	B	C
1	AKG_2_80_NoPep		
2	Wavelength (nm)	Wavenumber (1/cm)	Abs
3	800	12500.0	0.092
4	799	12515.6	0.092
5	798	12531.3	0.093
6	797	12547.1	0.093
7	796	12562.8	0.093
8	795	12578.6	0.094
9	794	12594.5	0.094
10	793	12610.3	0.094
11	792	12626.3	0.095

Step 3

AKG_2_80_exp.xls

Search in Sheet

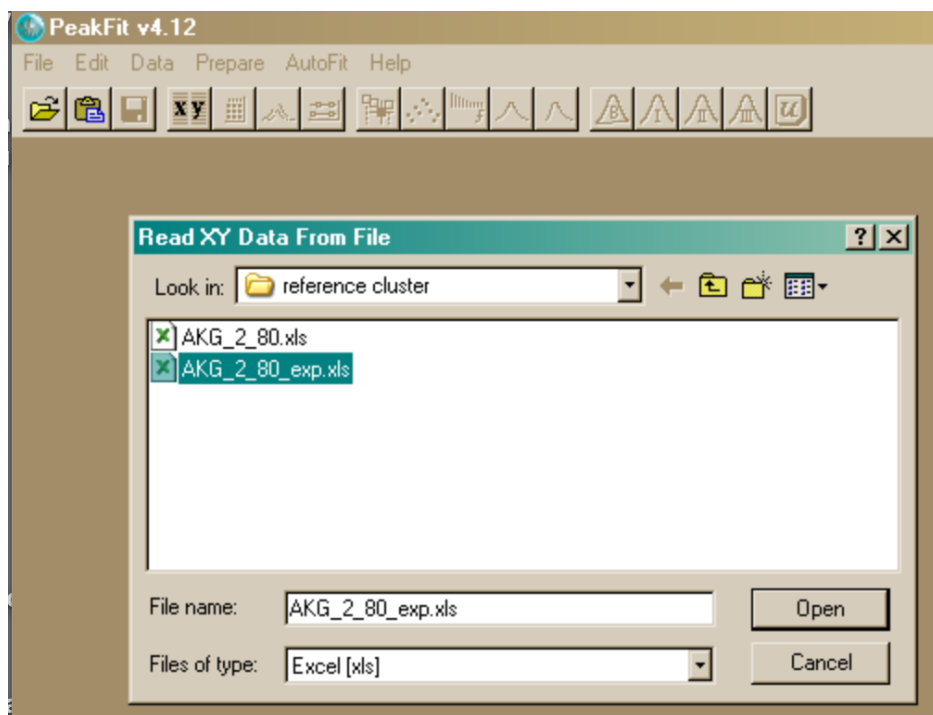
Home Layout Tables Charts SmartArt Formulas Data

Paste Arial 10 Number Conditional Formatting Styles

B9 0.0943158716

	A	B
1	AKG_2_80_NoPep	
2	Wavenumber	Abs
3	12500.0	0.092
4	12515.6	0.092
5	12531.3	0.093
6	12547.1	0.093
7	12562.8	0.093

Step 4



Select Columns for X-Y Data Table

File: Z:\Desktop\UV-vis fits\reference cluster\AKG_2_80_exp.xls
Format: Excel XLS OLE

X Column: AIA : AKG_2_80_NoPep Wavenumber (1/cm)
Y Column: AIB : Abs
W Column:

Select Column: X Values Y Values Weights

- AIA : AKG_2_80_NoPep Wavenumber (1/cm)
- AIB : Abs

OK
Cancel
Help

Data Description and Variable Names

File Source: Z:\Desktop\UV-vis fits\reference cluster\AKG_2_80_exp.xls
Number of XY in Table: 601

Main Title: AKG_2_80_NoPep
X Title: Wavenumber (1/cm)
Y Title: Abs

OK Previous Titles Help

AKG_2_80_NoPep

Nov 6, 2019 10:53:30 PM Pentium
Mem: 2048.000 2735.395 FPI: 1234010
#X:Y: 601 Active: 601
z:\desktop\uv-vis fits\reference

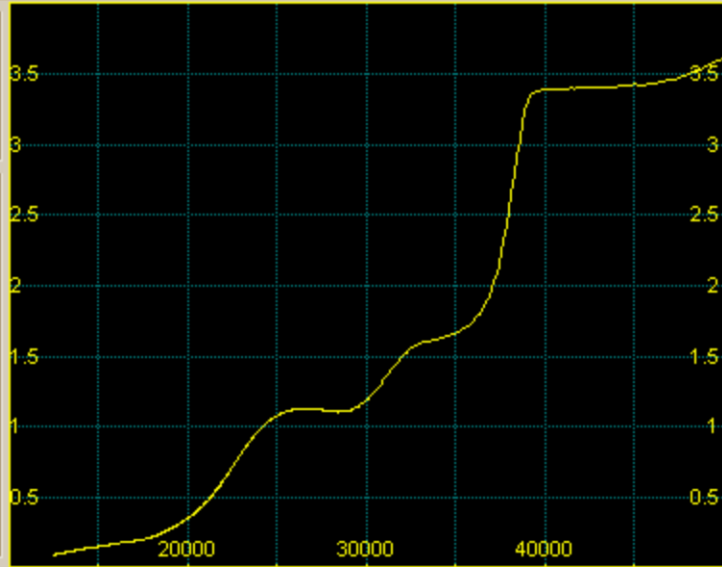
X Variable: Wavenumber (1/cm)

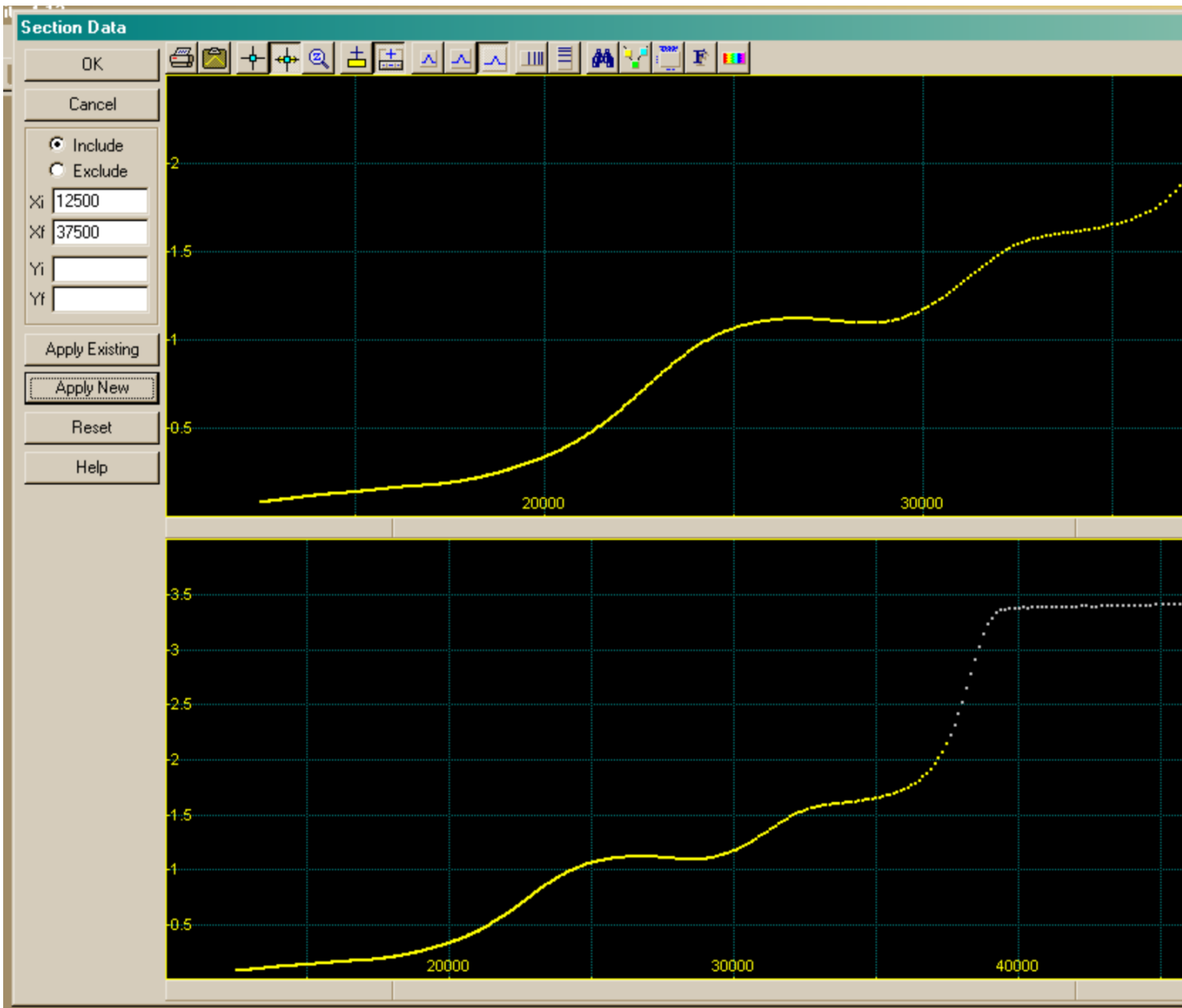
Min: 1.25e+04 Max: 5e+04
Range: 3.75e+04 Median: 2e+04
Mean: 2.31e+04 Std: 9.58e+03
atYmin: 1.25e+04 atYmax: 5e+04

Y Variable: Abs

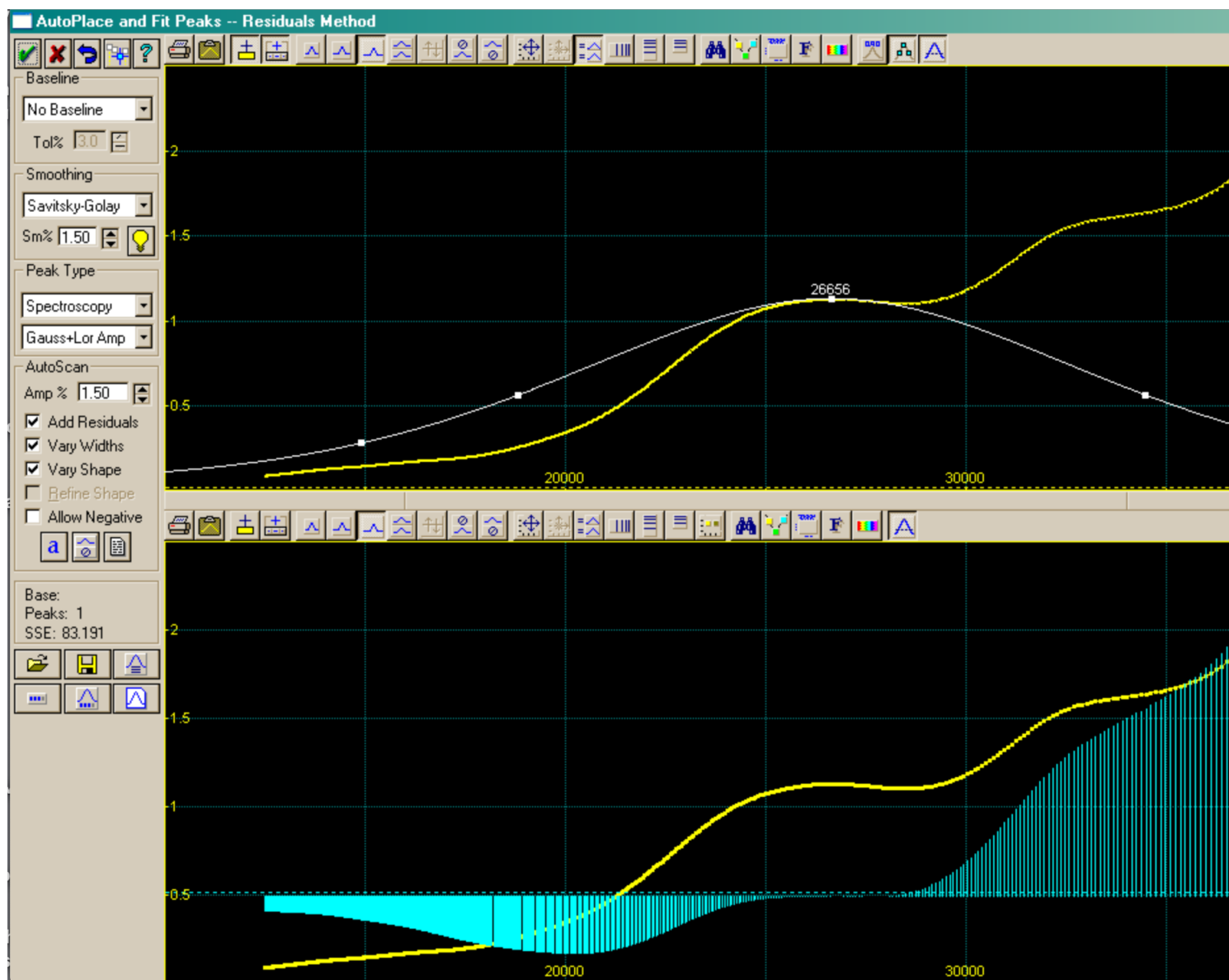
Min: 0.092211 Max: 3.609916
Range: 3.517705 Median: 0.348227
Mean: 0.869902 Std: 1.006532
atXmin: 0.092211 atXmax: 3.609916

Area Xmin to Xmax: 64527.956

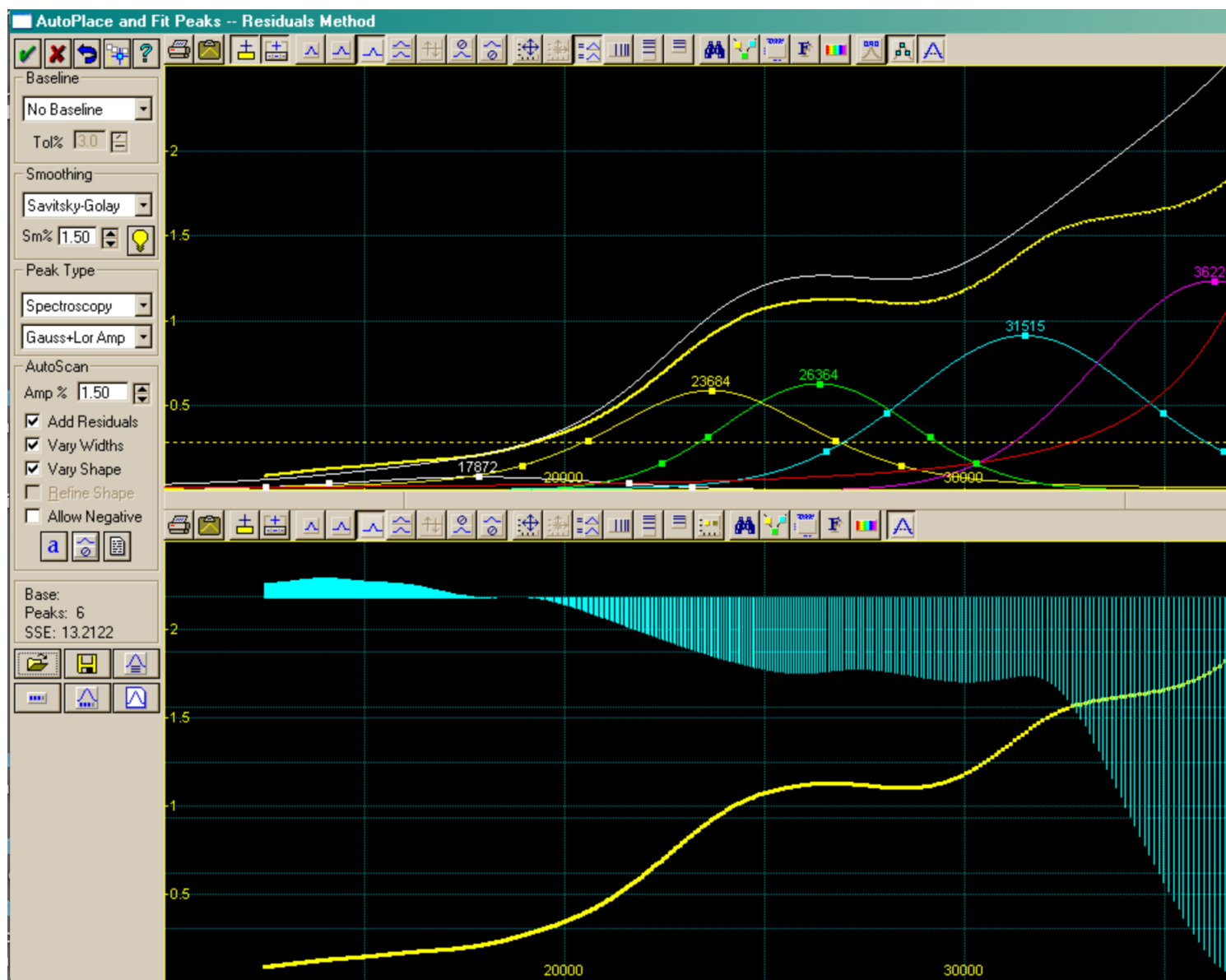




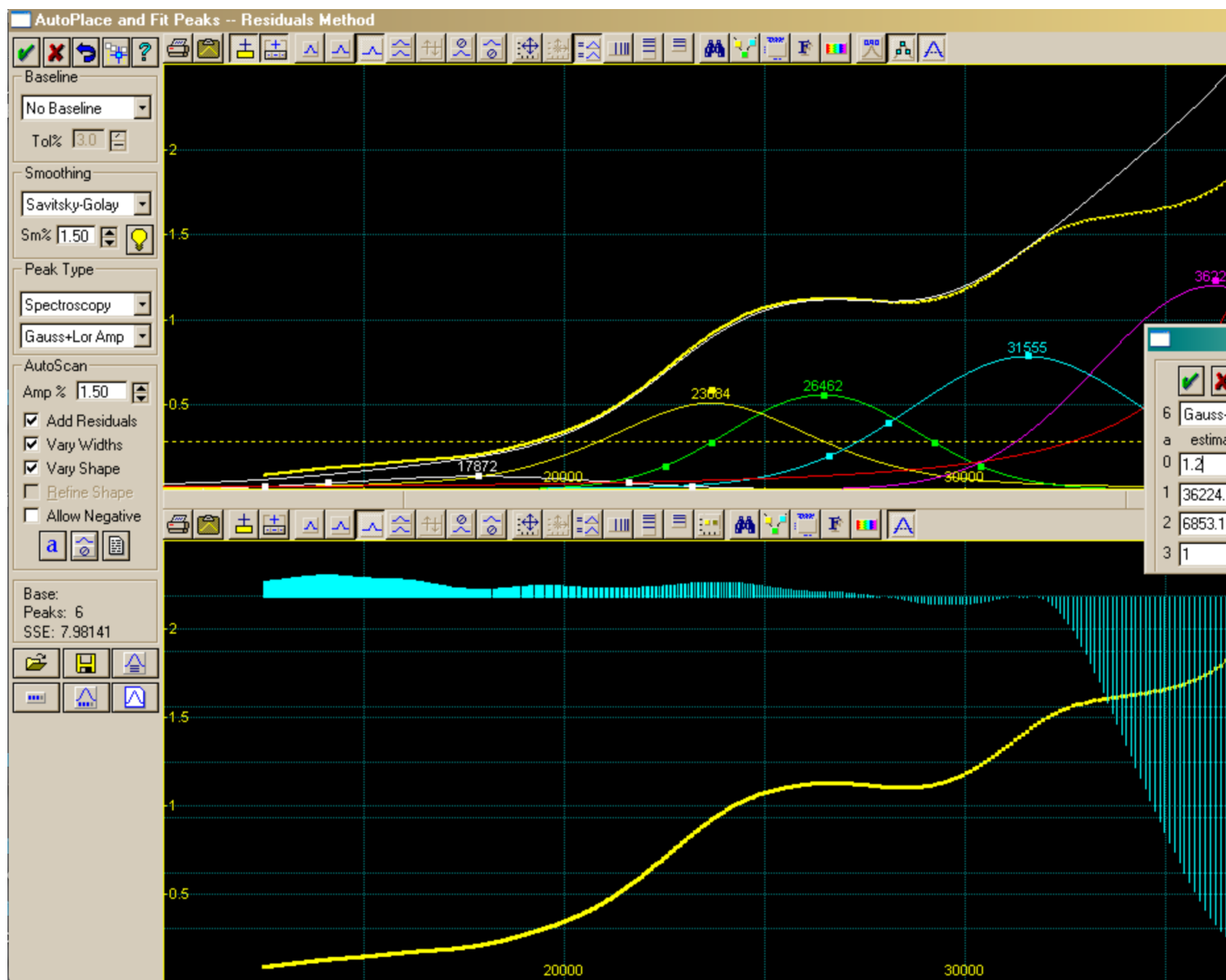
Step 5



Step 6



Step 7

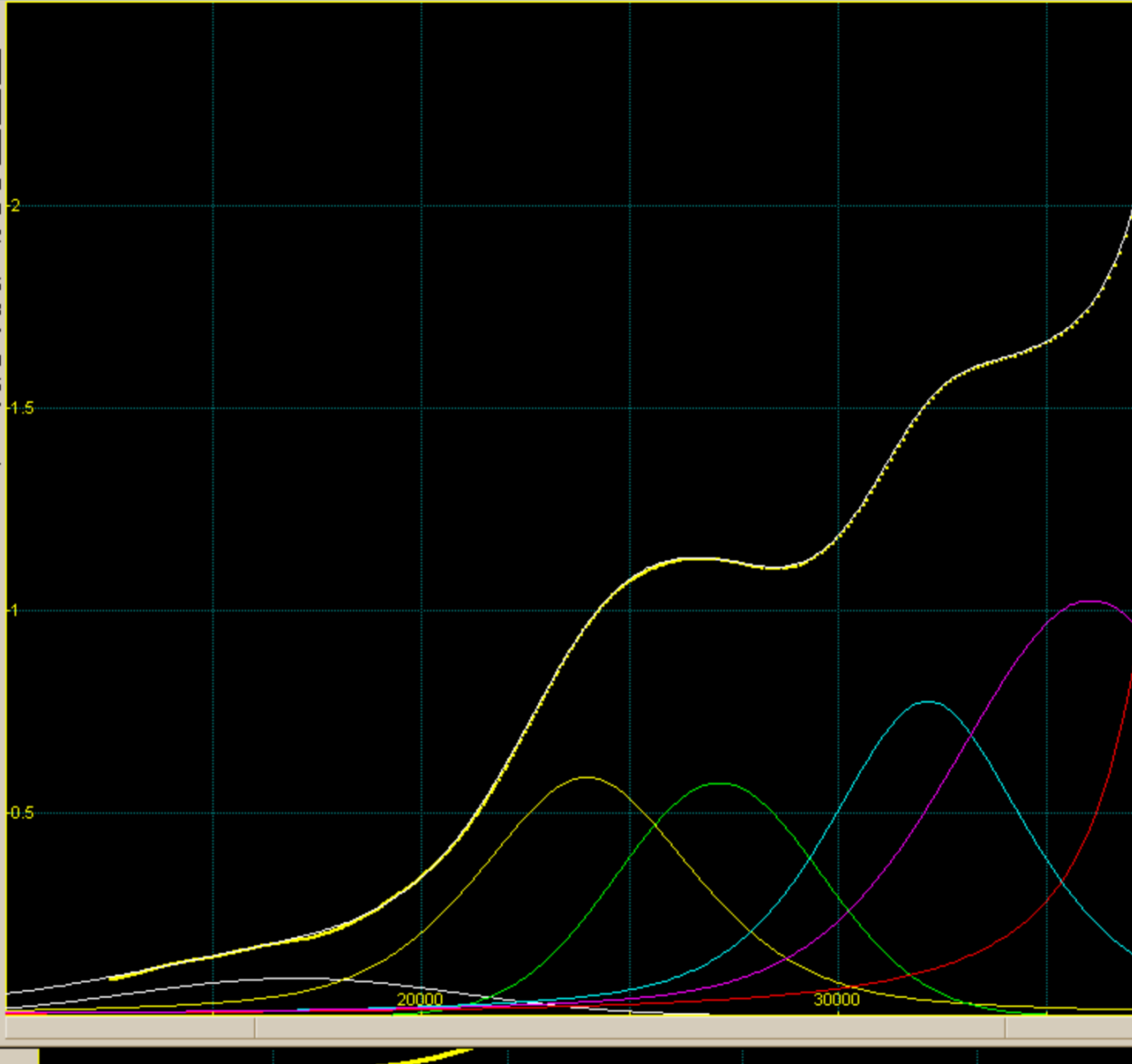


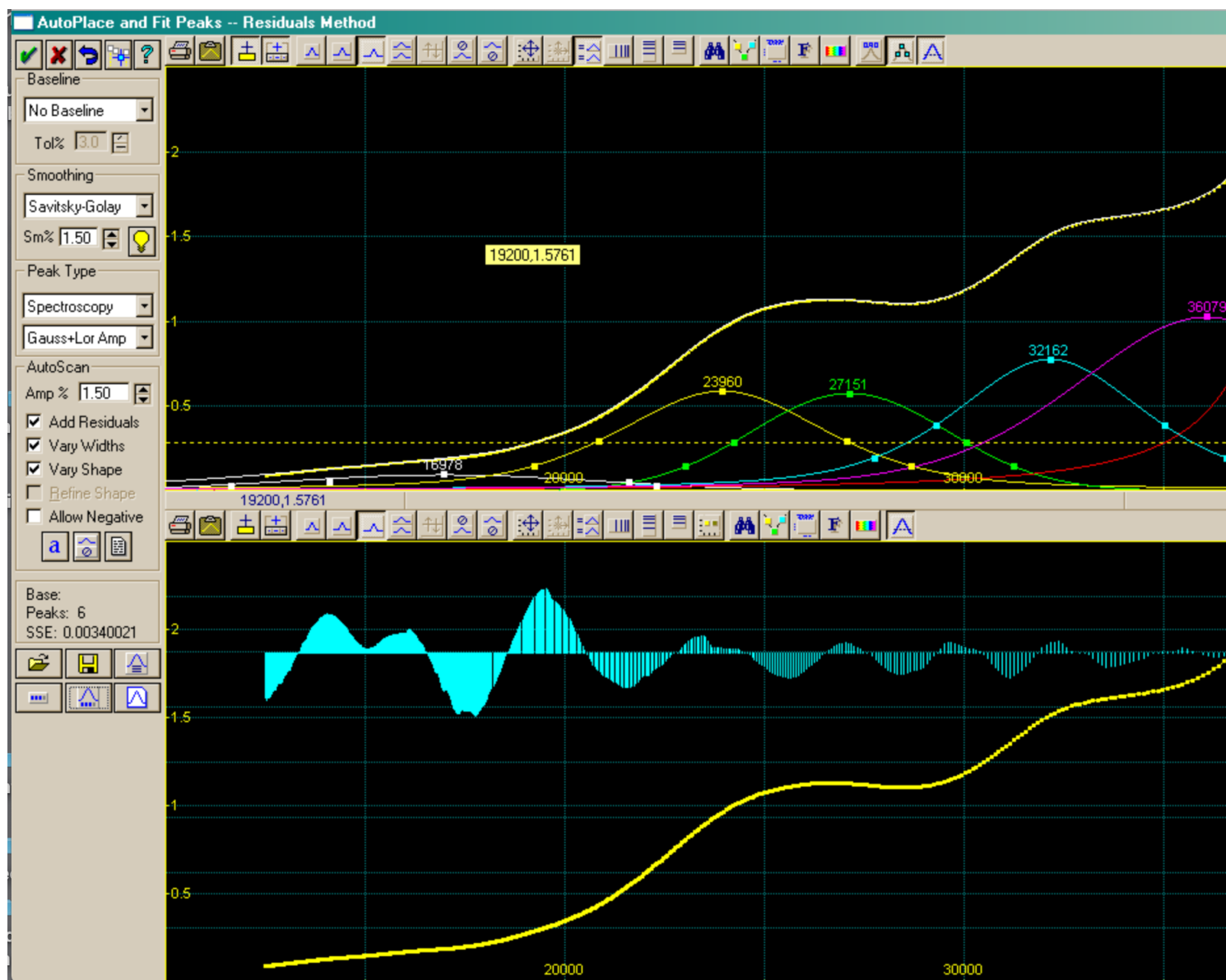
Step 8

PeakFit Graphical Fitting

- Abort Fit
- Addl Adjust
- Review Fit

Iter: 10000
Constraints: 0
Merit: 0.0034002
SdErr: 0.0025821
Fstat: 9.575e+05
 r^2 : 0.99998
Time: 28.87
Time/Iter: 0.00
Evl: 32279995
Evl/Iter: 3227
Data: 534/1
Parms: 24
 Iter Update





Step 9

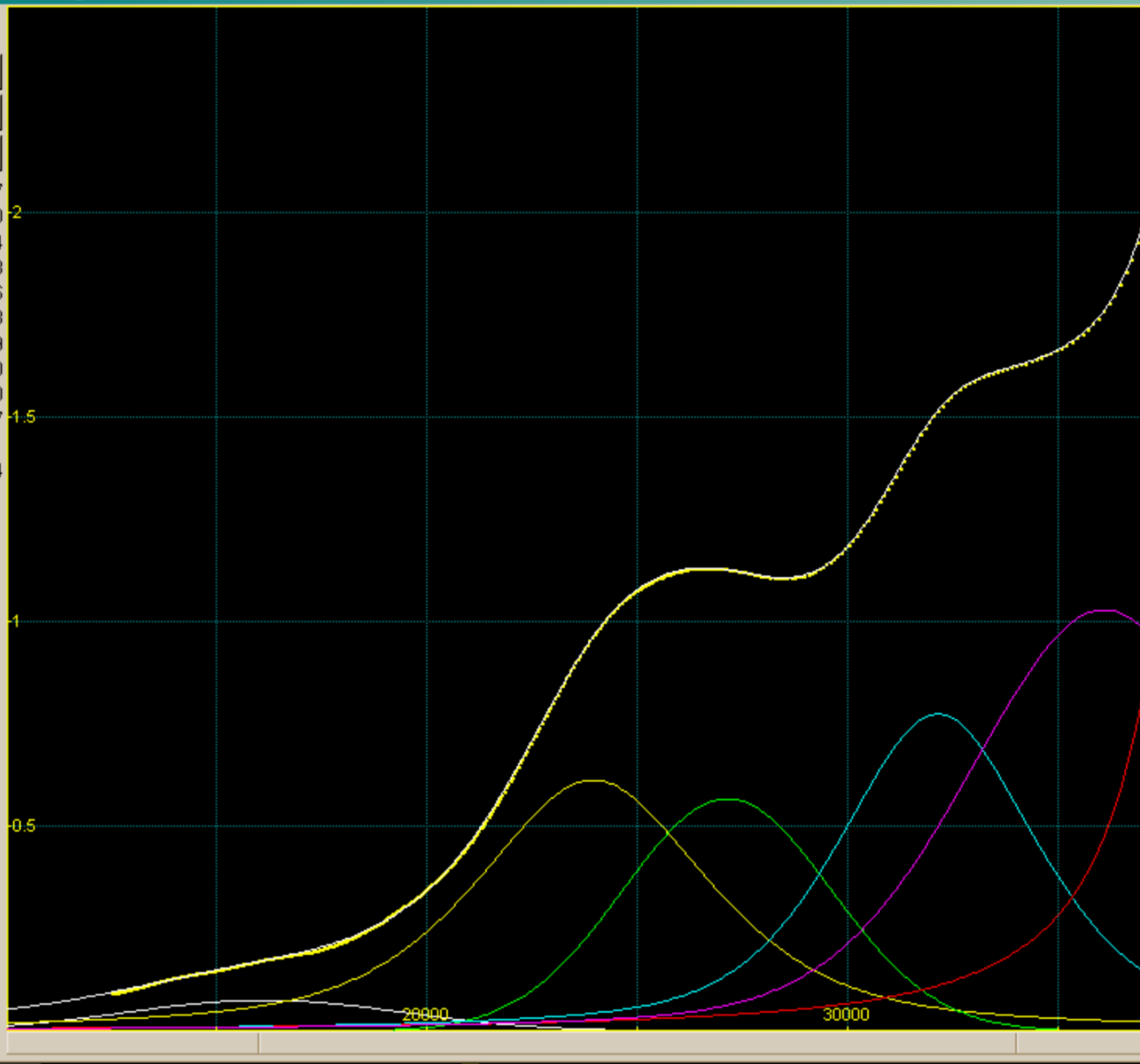
PeakFit Graphical Fitting

Abort Fit

Addl Adjust

Review Fit

Iter: 2697
Constraints: 0
Merit: 0.0028484
SdErr: 0.0023633
Fstat: 1.143e+06
r: 0.99998
Time: 8.29
Time/Iter: 0.00
Evl: 8705890
Evl/Iter: 3227
Data: 534/1
Parms: 24
 Iter Update



Step 10

Review Fit



- OK
- Export
- Numeric
- Data
- Eval
- Residuals
- Help

AKG 2 80 NoPep

Print Graph



PSI PostScript
FILE:

- Half-Page (Portrait)
- Full-Page (Landscape)
- Custom Portrait
- Custom Landscape

- Frame Graph
- Use Color
- Add Numeric Summary

Margins

Left:

Above:

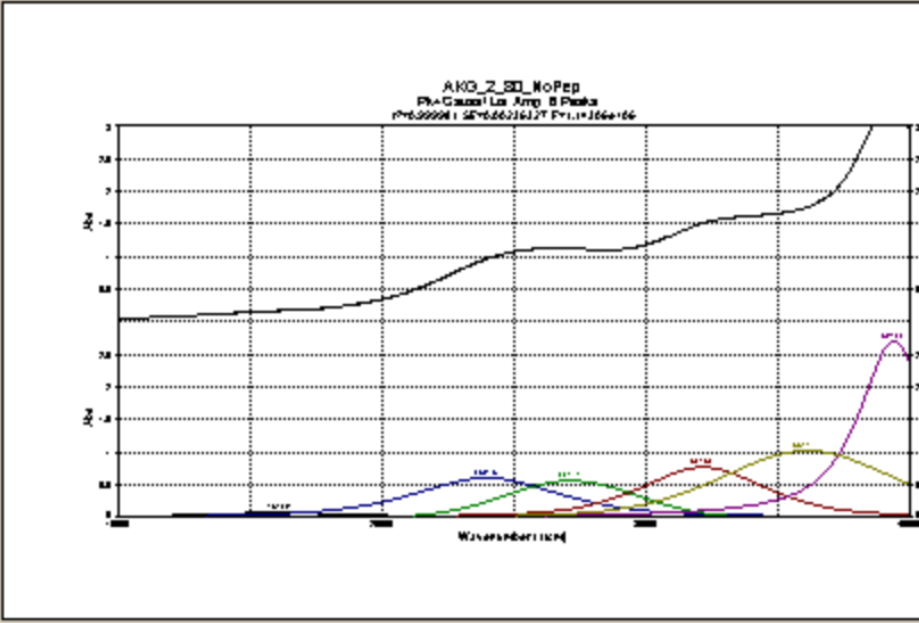
Right:

Below:

inches cm

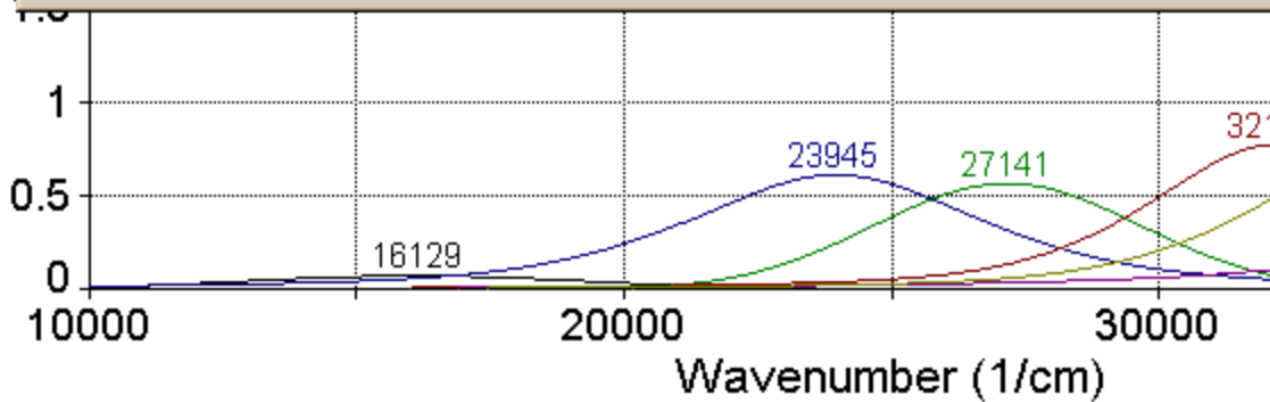
Font %:

Line Wid:



Abs

Abs



Export Peak Fit [X]

Format:

- ASCII
- Lotus 123 WK3
- Excel XLS
- Quattro Pro WB1
- SigmaPlot SP5

Generated Data:

X Start:

X Incr:

X End:

OK

Cancel

Help

Peak Summary

File Edit Style Options

Description: AKG_2_80_NoPep

X Variable: Wavenumber (1/cm)

Y Variable: Abs

File Source: z:\desktop\uv-vis fits\reference cluster\akg_2_80_exp.xls

Fitted Parameters

r ²	Coef Det	DF	Adj r ²	Fit Std Err	F-value
0.99998060			0.99997969	0.00236327	1.1431e+06

Peak	Type	a ₀	a ₁	a ₂	a ₃
1	Gauss+Lor Amp	0.07609162	16129.2685	7768.26935	1.00000000
2	Gauss+Lor Amp	0.61292434	23944.9075	6617.86443	0.28804748
3	Gauss+Lor Amp	0.56701024	27140.9673	5866.21741	1.00000000
4	Gauss+Lor Amp	0.77421383	32159.9429	5616.75369	0.37520359
5	Gauss+Lor Amp	1.02889287	36114.0748	7724.55518	0.62936128
6	Gauss+Lor Amp	2.70949883	39404.7716	3185.30560	0.07686268

Measured Values

Peak	Type	Amplitude	Center	FWHM	Asym50	FW Base	Asym
1	Gauss+Lor Amp	0.07609162	16129.2685	7768.26935	1.00000000	15549.8087	1.0000
2	Gauss+Lor Amp	0.61292434	23944.9075	6617.86443	1.00000000	17537.0791	1.0000
3	Gauss+Lor Amp	0.56701024	27140.9673	5866.21741	1.00000000	11742.4557	1.0000
4	Gauss+Lor Amp	0.77421383	32159.9429	5616.75369	1.00000005	14055.1322	1.0000
5	Gauss+Lor Amp	1.02889287	36114.0748	7724.55518	1.00000002	17110.2955	1.0000
6	Gauss+Lor Amp	2.65487066	39172.4233	0.00000000	-1.00000000	10214.7796	1.1078

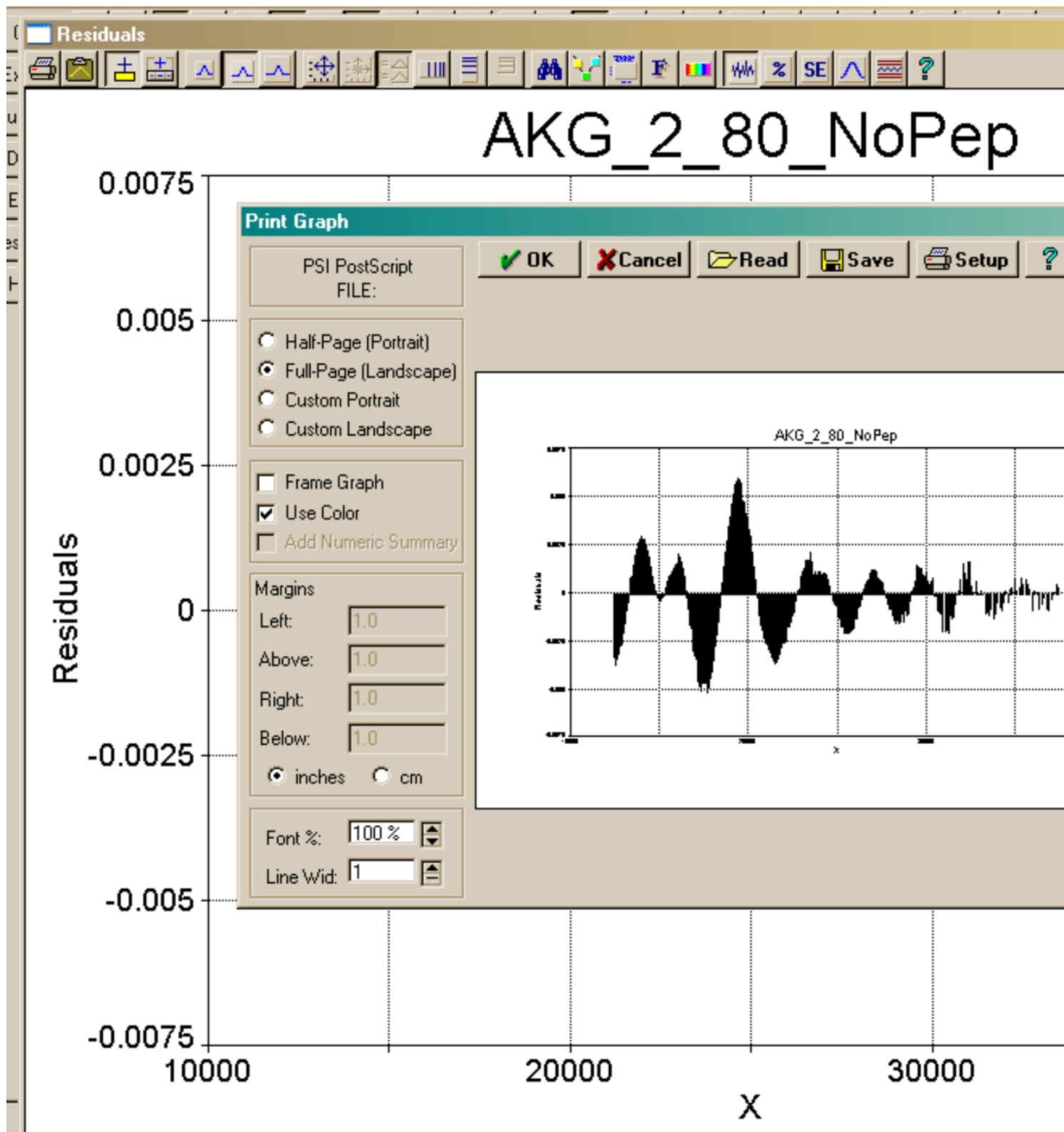
Peak	Type	Anlytc Area	% Area	Int Area	% Area	Centroid	Mome
1	Gauss+Lor Amp	629.206628	1.64470306	543.865428	1.88062468	16960.5686	7.1745
2	Gauss+Lor Amp	5603.75065	14.6478207	4941.22768	17.0862023	24076.6016	1.641e
3	Gauss+Lor Amp	3540.63589	9.25497989	3540.57427	12.2429024	27140.7784	6.2039
4	Gauss+Lor Amp	5796.25189	15.1510057	5041.59639	17.4332659	31355.5321	1.3083
5	Gauss+Lor Amp	9607.98653	25.1146192	5956.63821	20.5973762	33593.0675	1.2594
6	Gauss+Lor Amp	13078.7171	34.1868714	8895.50088	30.7596285	37058.8639	1.1871
	Total	38256.5487	100.000000	28919.4029	100.000000		

Parameter Statistics

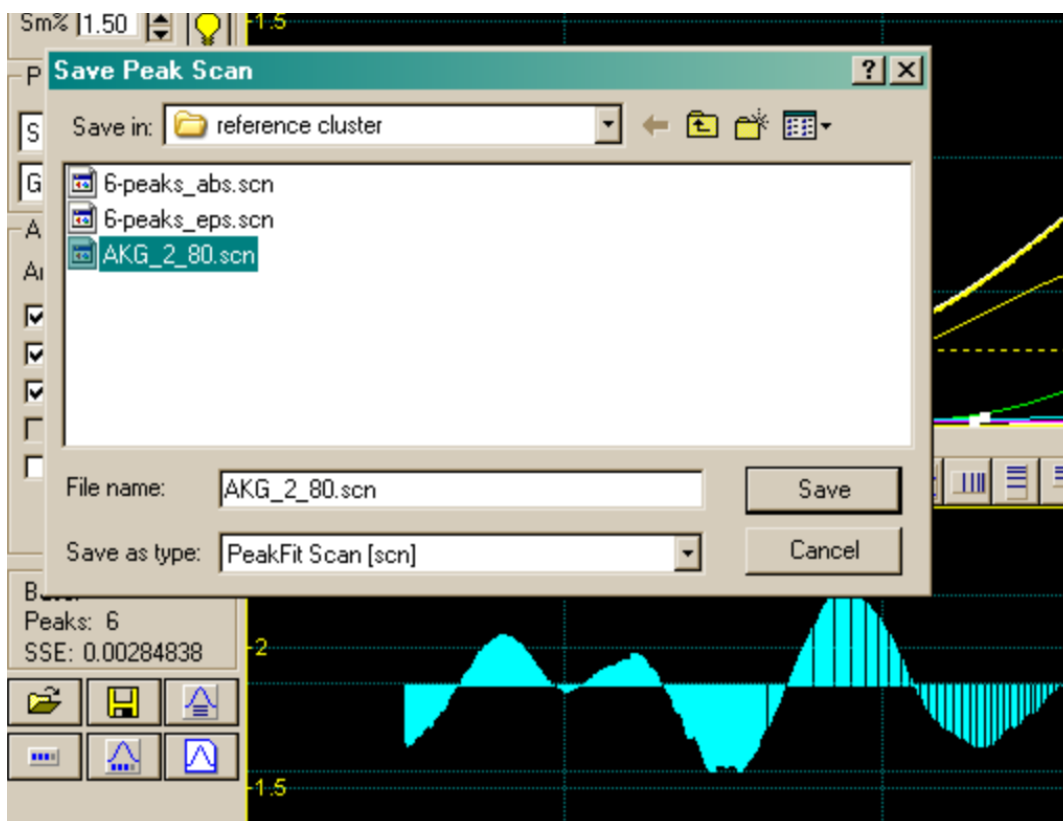
Data Summary

File Edit Style Type

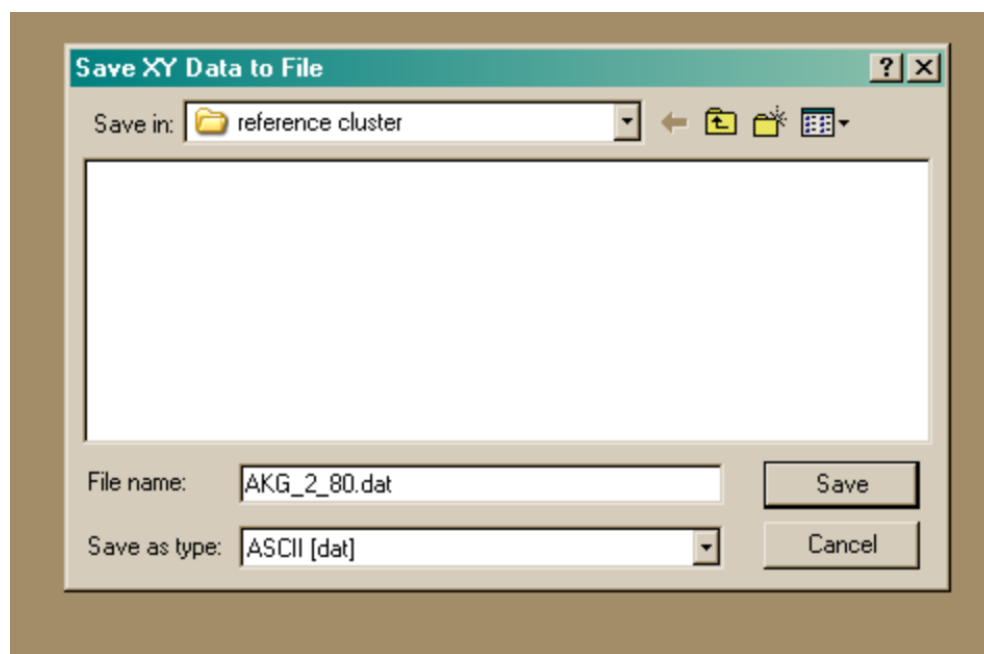
XY	*	X Value	Y Value	Y Predict	Residual	Residual%	95% Confidence Limits	
1		1.25e+04	0.0922111	0.0954891	-0.003278	-3.554857	0.0942211	0.0967570
2		1.252e+04	0.0924285	0.0958145	-0.003386	-3.663423	0.0945932	0.0970359
3		1.253e+04	0.0929602	0.0961414	-0.003181	-3.422145	0.0949650	0.0973178
4		1.255e+04	0.0926609	0.0964696	-0.003809	-4.110324	0.0953366	0.0976026
5		1.256e+04	0.0930951	0.0967992	-0.003704	-3.978868	0.0957079	0.0978905
6		1.258e+04	0.0937313	0.0971302	-0.003399	-3.626166	0.0960790	0.0981813
7		1.259e+04	0.0943159	0.0974625	-0.003147	-3.336291	0.0964498	0.0984753
8		1.261e+04	0.0941338	0.0977963	-0.003662	-3.890659	0.0968202	0.0987723
9		1.263e+04	0.0946865	0.0981314	-0.003445	-3.638127	0.0971903	0.0990724
10		1.264e+04	0.0950180	0.0984678	-0.003450	-3.630734	0.0975600	0.0993757
11		1.266e+04	0.0956483	0.0988057	-0.003157	-3.300991	0.0979293	0.0996821
12		1.267e+04	0.0961663	0.0991449	-0.002979	-3.097340	0.0982982	0.0999916
13		1.269e+04	0.0964012	0.0994855	-0.003084	-3.199455	0.0986667	0.1003043
14		1.271e+04	0.0965971	0.0998275	-0.003230	-3.344264	0.0990348	0.1006202
15		1.272e+04	0.0976086	0.1001709	-0.002562	-2.625037	0.0994024	0.1009393
16		1.274e+04	0.0978061	0.1005156	-0.002710	-2.770327	0.0997696	0.1012616
17		1.276e+04	0.0977493	0.1008617	-0.003112	-3.184054	0.1001364	0.1015870
18		1.277e+04	0.0980521	0.1012092	-0.003157	-3.219812	0.1005028	0.1019156
19		1.279e+04	0.0990524	0.1015581	-0.002506	-2.529661	0.1008689	0.1022472
20		1.28e+04	0.0997040	0.1019083	-0.002204	-2.210802	0.1012345	0.1025820
21		1.282e+04	0.0994722	0.1022599	-0.002788	-2.802409	0.1016000	0.1029198
22		1.284e+04	0.0999869	0.1026128	-0.002626	-2.626247	0.1019651	0.1032605
23		1.285e+04	0.1007259	0.1029671	-0.002241	-2.225109	0.1023301	0.1036041
24		1.287e+04	0.1012644	0.1033228	-0.002058	-2.032723	0.1026951	0.1039506
25		1.289e+04	0.1012017	0.1036799	-0.002478	-2.448727	0.1030600	0.1042997
26		1.29e+04	0.1013629	0.1040383	-0.002675	-2.639387	0.1034250	0.1046515
27		1.292e+04	0.1018209	0.1043980	-0.002577	-2.531026	0.1037902	0.1050058
28		1.294e+04	0.1027640	0.1047592	-0.001995	-1.941515	0.1041557	0.1053626
29		1.295e+04	0.1028393	0.1051216	-0.002282	-2.219329	0.1045216	0.1057217
30		1.297e+04	0.1034563	0.1054855	-0.002029	-1.961357	0.1048879	0.1060830
31		1.299e+04	0.1037717	0.1058506	-0.002079	-2.003363	0.1052549	0.1064464
32		1.3e+04	0.1046304	0.1062172	-0.001587	-1.516557	0.1056225	0.1068118
33		1.302e+04	0.1046714	0.1065850	-0.001914	-1.828195	0.1059908	0.1071792
34		1.304e+04	0.1050797	0.1069542	-0.001875	-1.783952	0.1063601	0.1075484



Step 11



Step 12



Step 13

						[Fe ₄ S ₄ (SEt) ₄] ²⁻	[Fe ₄ S ₄ (BME) ₄] ²⁻	PFL-AE enzyme	avg. %	σ, %	target 90 μM
					Integrated area	196792	191439	17401			loading
4536	5110	7151	Maquette FdM-7_AKG51-53 peptide-free reconstitution	Sequence CIACGAC	16797	85.4	87.7	86.9	86.7 ±	1.2	96.3%
4941	3541	5042	AKG_2_80	no peptide	13523	68.7	70.6	69.9	69.8 ±	1.0	77.5%

AKG_2_80.rtf — Edited

Courier New Regular 12 B I U 1.0

3	Gauss+Lor	Amp	0.56701024	27140.9673	5866.21741	1.00000000	11742.4557	1.00000000
4	Gauss+Lor	Amp	0.77421383	32159.9429	5616.75369	1.00000005	14055.1322	1.00000002
5	Gauss+Lor	Amp	1.02889287	36114.0748	7724.55518	1.00000002	17110.2955	1.00000001
6	Gauss+Lor	Amp	2.65487066	39172.4233	0.00000000	-1.00000000	10214.7796	1.10787947
Peak	Type		Anlytc Area	% Area	Int Area	% Area	Centroid	Moment2
1	Gauss+Lor	Amp	629.206628	1.64470306	543.865428	1.88062468	16960.5686	7.1745e+06
2	Gauss+Lor	Amp	5603.75065	14.6478207	4941.22768	17.0862023	24076.6016	1.641e+07
3	Gauss+Lor	Amp	3540.63589	9.25497989	3540.57427	12.2429024	27140.7784	6.2039e+06
4	Gauss+Lor	Amp	5796.25189	15.1510057	5041.59639	17.4332659	31355.5321	1.3083e+07
5	Gauss+Lor	Amp	9607.98653	25.1146192	5956.63821	20.5973762	33593.0675	1.2594e+07
6	Gauss+Lor	Amp	13078.7171	34.1868714	8895.50088	30.7596285	37058.8639	1.1871e+07
	Total		38256.5487	100.000000	28919.4029	100.000000		